ALGERIAN JOURNAL OF ENGINEERING AND TECHNOLOGY

Algerian Journal of Engineering and Technology
ISSN: 2716-9227 (Print)
EISSN: 2716-9278 (Online)
DOI: https://doi.org/10.57056/ajet.v9i1.162
Benaskeur et al / vol. 09, n°1 - 2024

Original Article **Open Access**

GaAs electrical-properties enhancement by neutron transmutation doping

Naziha Benaskeur* and Mohamed Hachouf

Nuclear Research Centre of Birine, BP 180, Ain Oussera, Djelfa, Algeria

* Corresponding author. E-mail address: *n.hachouf@crnb.dz*
Article history: Received 16 April 2024, Revised 22 June 2024, Accepted 25 June 2024

ABSTRACT

This study investigates the potential of neutron transmutation doping (NTD) for enhancing the electrical uniformity of gallium arsenide (GaAs) wafers used in photovoltaic cells. Uniformity is crucial for improving solar cell efficiency, which is a key objective in solar power engineering. We employ the SCALE6.1 code to simulate the impact of NTD on the Radial Resistivity Gradient (RRG) within GaAs wafers for various neutron fluence values. The results demonstrate a clear decrease in RRG with increasing neutron fluence. Notably, acceptable RRG values (below 5%) are achievable for both high (25 Ω.cm) and low (5 Ω.cm) initial resistivity GaAs wafers with moderate neutron fluence levels ($7.25x10^{14}$ n/cm² and $3.63x10^{15}$ n/cm², respectively). This suggests that NTD can effectively improve the electrical properties of GaAs, leading to potentially higher solar cell efficiency.

Keywords: Neutron transmutation, Fluence, SCALE6.1, RRG, GaAs.

Graphical abstract

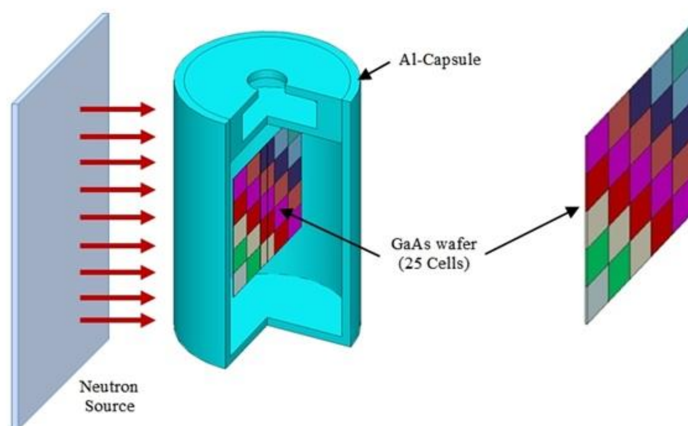

SCALE6.1 modeled system.

Recommended Citation
Benaskeur N, Hachouf M. GaAs electrical-properties enhancement by neutron transmutation doping. *Alger. J. Eng. Technol. 2024, 9(1): 75-83.* https://doi.org/10.57056/ajet.v9i1.162

© 2024 The Authors. Published by University of El Oued. This is an open access article under the CC BY-NC license (https://creativecommons.org/licenses/by-nc/4.0/). Available at: https://www.jetjournal.org/index.php/ajet/index

1. Introduction

Solid-state materials irradiated with thermal neutrons have garnered significant attention for use in potential applications. Due to the high penetrating power of neutrons, neutron-transmutation doping (NTD) is a specialized technique for semiconductor doping with precise control of dopant concentration and uniform distribution [1-4]. This method relies on the capture of thermal neutrons by nuclei within the solide-state material lattice of the primary semiconductor material. The effectiveness of this process depends on capture cross-sections and natural isotope abundances in the irradiated sample.

Gallium arsenide (GaAs) stands as one of the most widely used III-V semiconductor-compounds in photovoltaic applications. It is well known by its high electron mobility and direct band gap. Single-junction GaAs devices can achieve efficiencies approaching 30%. Due to their adequate electrical and thermal properties, GaAs solar cells have been extensively studied and have rapidly become a reference system for thin-film solar cells [5].

In contrast to silicon, GaAs's direct bandgap enhances light absorption. This characteristic allows producing thin and flexible solar cells ideal for weight-sensitive applications where high efficiency is needed. However, the high manufacturing cost of GaAs solar cells, makes their widespread adoption significantly expansive compared to silicon-based technology [6].

The ongoing enhancement of the electrical properties of semiconductor-based photovoltaic cells constitutes a research area of great interest. In the frame of this objective, this study proposes the NTD application to achieve a uniform distribution of electrical resistivity within doped GaAs semiconductors.

This study aims to simulate neutron transmutation doping (NTD) conditions of GaAs used in photovoltaic cells. The SCALE6.1 code system [7] is used to model and simulate the radial homogenization of dopants within the GaAs wafer after irradiation under different neutron fluences. Based on the simulated reaction rate values, which allow us to determine the dopant concentration produced within the irradiated target, the final resistivity distribution can be calculated and the predicted enhancement is established.

2. Neutron transmutation doping of GaAs

The NTD of silicon semiconductor in thermal neutron flux was reported by Tanenbaum and Mills [1]. This method has become a commercially viable process for producing bulk silicon with exceptionally uniform dopant distribution. Due to the challenges of achieving a uniform and precisely controlled dopant profile using traditional methods, NTD is particularly attractive for GaAs which is a promising material for high-efficiency solar cells.

Following the pioneering work by Mirianashvili and Nanobashvili (1971) on NTD of GaAs [2], significant research interest has emerged in this field [8-12]. These studies have demonstrated the effectiveness of NTD in achieving precise dopant concentrations in GaAs. The process relies on thermal neutron capture reactions with the main isotopes of GaAs, as shown below:

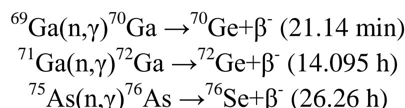

$$^{69}Ga(n,\gamma)^{70}Ga \rightarrow ^{70}Ge+\beta^{-} \text{ (21.14 min)}$$
$$^{71}Ga(n,\gamma)^{72}Ga \rightarrow ^{72}Ge+\beta^{-} \text{ (14.095 h)}$$
$$^{75}As(n,\gamma)^{76}As \rightarrow ^{76}Se+\beta^{-} \text{ (26.26 h)}$$

The Se and Ge produced by NTD have different impacts on the electrical properties of GaAs. Se acts as a deep donor with an energy level close to the conduction band, contributing to n-type conductivity. Ge, on the other hand, can behave as a shallow donor if located on a Ga site or as an acceptor (Ev+0.04 eV) if located on an As site. Since most of the NTD-doped Se and a portion of the Ge are expected to act as donors, neutron transmutation doping is predicted to favor n-type doping in GaAs [13].

3. Simulation Setup for NTD

This section describes the geometric modeling of the configuration used for simulating the NTD process in a gallium arsenide (GaAs) wafer for solar cell applications. The modeling is performed using the SCALE6.1 code.

3.1. Geometry description

The simulated configuration consists of a cuboid GaAs wafer (3x3x0.02 cm3) placed inside an aluminum (Al) capsule (Fig.

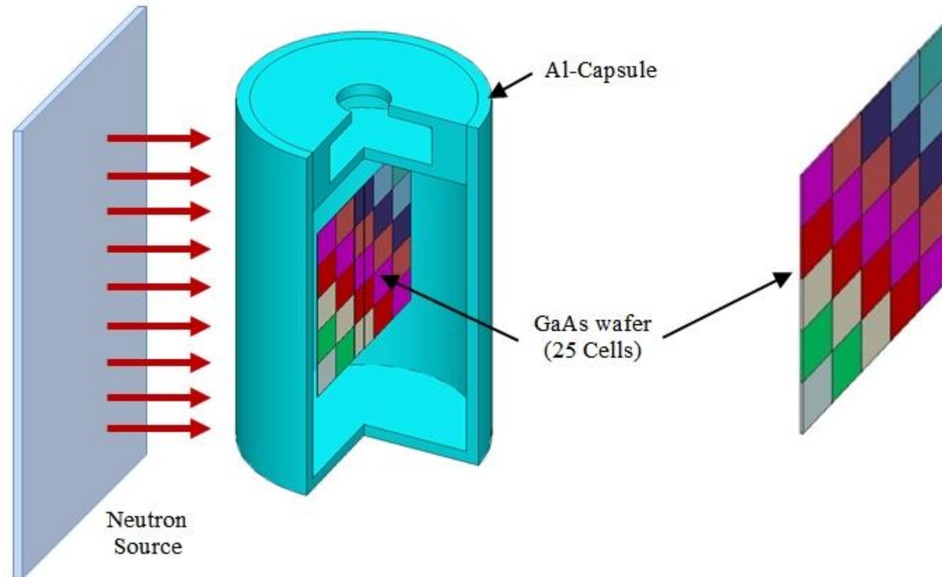

Fig 1. SCALE6.1 modeled system.

3.2. Material composition

The material composition of the GaAs wafer includes Ga-nat and As-nat as its primary elements, constituting the fundamental structure of GaAs. Si-nat atoms are introduced as dopant impurities to adjust the initial resistivity, which depends on their initial concentration. The mass fraction of Si-nat varies across the wafer to simulate a non-uniform initial resistivity distribution. Table 1 summarizes the composition of the studied GaAs semiconductor, highlighting the mass fraction and mass density of each element.

Table 1. Composition of the studied GaAs semiconductor

Composition	**Mass fraction (%)**	**Mass density (g/cm^3)**
Si-nat (variable)	$(2.58\text{-}12.92)\times10^{-8}$	
Ga-nat	48.203	5.31
As-nat	51.797	

3.3. Neutron source

The neutron source used in this setup is a planar source positioned parallel to the GaAs wafer surface. This source emits neutrons in a single direction, perpendicular to the wafer surface, ensuring direct interaction with the GaAs material. This arrangement allows the modeling of unilateral neutron irradiation used in the NTD process. The used thermal neutron flux and fast neutron flux are respectively 1×10^{12} n/cm²·s and 1×10^{9} n/cm²·s. The ratio of these two neutrons flux is 1000, corresponding to typical NTD conditions as defined by the IAEA in 2012 [14].

To predict the neutron effects on GaAs, we employed the Monte Carlo simulation code SCALE6.1. This software enables precise simulation of reaction rates (reaction per second) which helps in the theoretical assessment of neutron fluence effects for a given irradiation time. The analysis of the integral reactions number depicts how neutron interactions progress during irradiation. This provides detailed information on the dopant behavior in the GaAs wafer under the used irradiation conditions.

This approach allowed us to predict theoretical outcomes before any physical experimentation, ensuring a comprehensive and rigorous study methodology.

4. Monte Carlo calculation methodology for dopant uniformity analysis

In order to study the radial uniformity of dopant concentration within the GaAs wafer after NTD, a Monte Carlo calculation methodology is employed. The process involves the following steps:

4.1. Cell division

To investigate the influence of an initial non-uniform dopant distribution with a 25% radial resistivity gradient across the wafer, the simulation assumes the GaAs wafers to be initially n-type doped with Si-nat. By virtually dividing the wafer into 25 smaller cells (Fig. 2), the simulation allows for a detailed analysis of how this non-uniformity is evolved during the NTD process.

N_1 →

1	0.984	0.96	0.9	0.888
1.024	1	0.984	0.96	0.9
1.046	1.024	1	0.984	0.96
1.084	1.046	1.024	1	0.984
1.112	1.084	1.046	1.024	1

← N_{25}

Fig 2. Normalized initial resistivity distribution map (Measuring points).

The initial resistivity of each cell ″*j*″ is calculated by multiplying the global average initial resistivity (ρ_i) of the GaAs material by the corresponding value from the normalized initial resistivity (N_j) as shown in the distribution map (Fig. 2):

$$\rho_{ij} = \rho_i \times N_j \qquad ; j = 1, 2, \ldots, 25 \quad (1$$

where ρ_{ij} is the initial resistivity of the GaAs wafer in the cell ″*j*″ (Ω.cm).

4.2. Initial dopant concentration calculation

To determine the initial dopant concentration for each cell of GaAs (C_{ij}), Equation 2 is used, taking into account parameters such as the initial resistivity of the GaAs material in the cell ″j″ (ρ_{ij}) and the mobility of charge carriers:

$$C_{ij} = \frac{1}{\rho_{ij} \times q \times (\mu_e + \mu_h)} \quad (2$$

where:

C_{ij}: the initial dopant concentration in the cell ″*j*″ (atoms/cm³).
μ_e: the electron mobility at 300 K (8500 cm^2/Vs) [15].
μ_h: the hole mobility at 300 K (350 cm^2/Vs) [15].
q: the elementary charge (1.6×10^{-19}C).

It is assumed that the initial dopant present in the GaAs wafer is silicon (Si-nat) (Table1). During the material definition in the SCALE6.1 code, the specific resistivity and the corresponding dopant concentration of each of 25 cells are accurately represented in the simulation model.

4.3. Dopant concentration produced by NTD

The SCALE6.1 code calculates the (n,γ) reaction rates in the GaAs material for each cell ″j″ (R_j), which involves the absorption of neutrons by Ga and As atoms, resulting in the formation of dopant atoms (Se and Ge). The dopant

concentration produced during NTD in each cell (C_{pj}) is calculated by multiplying the (n,γ) reaction rate (R_j) by the irradiation time (t_r), as shown in Equation 3:

$$C_{pj} = R_j + t_r \quad (3$$

where:
C_{pj} : the concentration of produced dopants in the cell ″*j*″ (atoms/cm³).
R_j : the (n,γ) reaction rate in the cell ″*j*″ (reactions/s).
t_r : the irradiation time (seconds).

4.4. Final dopant concentration calculation

The final dopant concentration in each cell (C_{fj}) is then determined by adding the corresponding initial dopant concentration (C_{ij}) to the dopant concentration produced by NTD (C_{pj}), as expressed in Equation 4:

$$C_{fj} = C_{ij} + C_{pj} \quad (4$$

where:
C_{fj} : the final dopant concentration in the cell ″*j*″ (atoms/cm³).

However, the (n,γ) reaction rate is a critical parameter influencing the final dopant concentration. By accurate modeling of these reaction rates, we can predict the dopant concentration distribution in the GaAs wafer, ensuring a precise and reliable analysis of the NTD process.

4.5. Final resistivity calculation after NTD

After irradiation, each cell will exhibit a final resistivity, contributing to an overall lower average resistivity of the GaAs wafer. The final resistivity of each cell (ρ_{fj}) is calculated using Equation 5, which incorporates the final dopant concentration of each cell (C_{fj}):

$$\rho_{fj} = \frac{1}{C_{fj} \times q \times (\mu_e + \mu_h)} \quad (5$$

Then, the average finale resistivity (ρ_f) can be obtained by Equation 6:

$$\rho_f = \frac{\sum_{j=1}^{n} \rho_{fj}}{n} \quad (6$$

where n is the number of cells.

This approach ensures a detailed and accurate assessment of the dopant uniformity, achieved through NTD, and its impact on the GaAs electrical properties.

5. Quantifying radial resistivity gradient

The radial resistivity gradient (RRG) is a metric used to quantify the non-uniformity in resistivity across the wafer. Equation 7 is used to calculate the RRG, by using the minimum ($\rho_{\min}$) and maximum ($\rho_{\max}$) resistivity values measured for all cells of the GaAs surface [14]:

$$RRG = \frac{(\rho_{\max} - \rho_{\min}) \times 100}{\rho_{\min}}, (\%) \quad (7$$

This metric is essential for evaluating how resistivity varies spatially within the wafer, directly influencing semiconductor performance. Maintaining an RRG within 5% aligns with typical customer requirements [14,17,18], ensuring consistent quality and reliability in semiconductor manufacturing and applications.

6. Results and discussion

6.1. Impact on Electrical Resistivity

Fig. 3 demonstrates the relationship between neutron fluence (a measure of neutron irradiation intensity) and the average electrical resistivity of the GaAs wafer. We observe a clear decrease in resistivity with increasing neutron fluence. This decrease is attributed to the increased dopant concentration produced by NTD (refer to step 4 of the methodology).

The initial resistivity of the GaAs wafer also plays a role. For wafers with higher initial resistivity (e.g., 25 Ω.cm), the decrease in resistivity is more significant compared to those with lower initial resistivity (e.g., 5 Ω.cm). This is because the NTD process introduces a larger relative change in dopant concentration for wafers with a lower initial concentration.

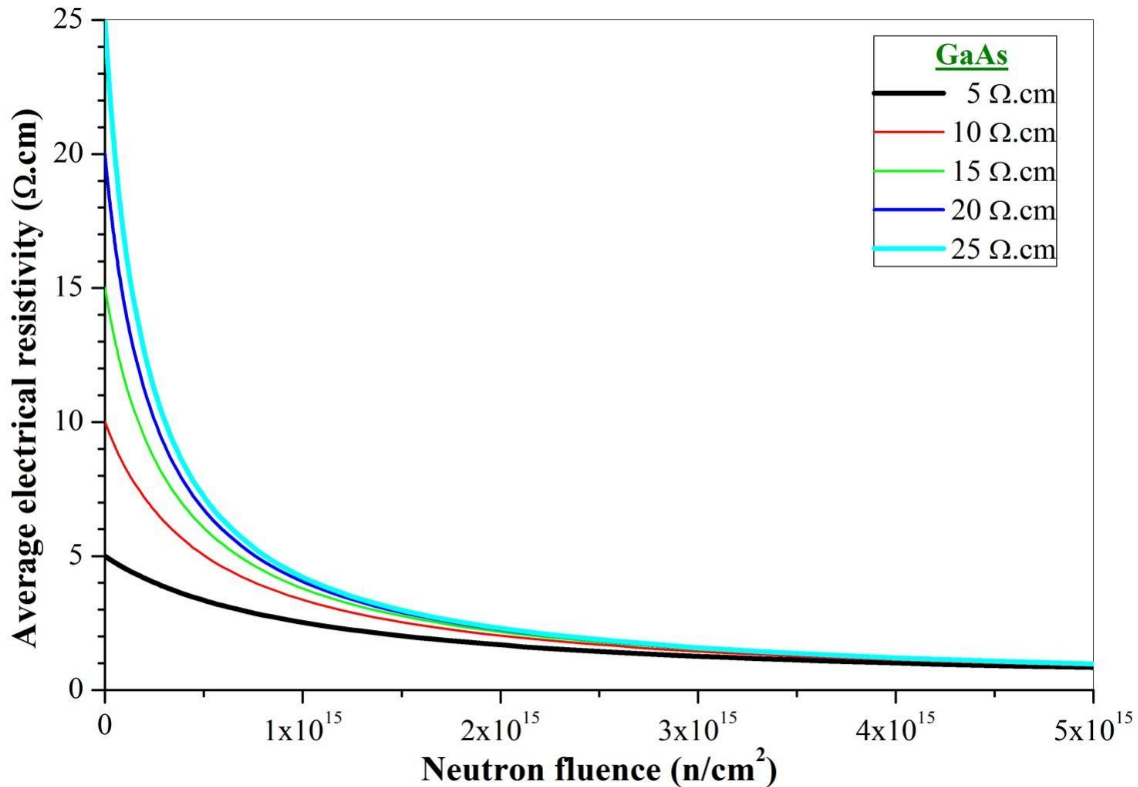

Fig. 3. GaAs electrical resistivity evolution as function of neutron fluence for various initial resistivities.

6.2. Impact on Radial Resistivity Gradient

Fig. 4 focuses on the Radial Resistivity Gradient (RRG), which reflects the uniformity of dopant concentration across the wafer's radius. The results show a significant decrease in RRG with increasing neutron fluence. This indicates that NTD effectively reduces the non-uniformity of the dopant distribution, leading to a more homogeneous concentration profile within the wafer. Notably, for neutron fluence exceeding $3x10^{15}$ n/cm², the average resistivity reaches a near-constant value around 2 Ω.cm (Fig. 3), suggesting a high degree of uniformity.

6.3. Optimizing NTD for different initial resistivities

The effectiveness of NTD for achieving a desired level of uniformity (low RRG) depends on the initial resistivity of the GaAs wafer, as confirmed in Fig. 4. To achieve an acceptable RRG value (below 5%), different neutron fluence levels are required for varying initial resistivity conditions.

For wafers with higher initial resistivity (such as 25 Ω.cm), a relatively low neutron fluence (F1 = $7.25x10^{14}$ n/cm²) is sufficient to achieve the target RRG value. This indicates a simpler and potentially less time-consuming NTD process for these wafers.

Conversely, wafers with lower initial resistivity (such as 5 Ω.cm) require a higher neutron fluence (F2 = $3.63x10^{15}$ n/cm²) to reach the same RRG target. While this might necessitate a slightly adjusted NTD treatment with a higher neutron

fluence, it's important to note that both fluence levels are achievable with moderate irradiation time. This highlights the adaptability of NTD; by adjusting the neutron fluence based on the initial resistivity, NTD can effectively improve the electrical uniformity of GaAs wafers across a range of resistivity values, potentially leading to enhanced performance in photovoltaic cell applications.

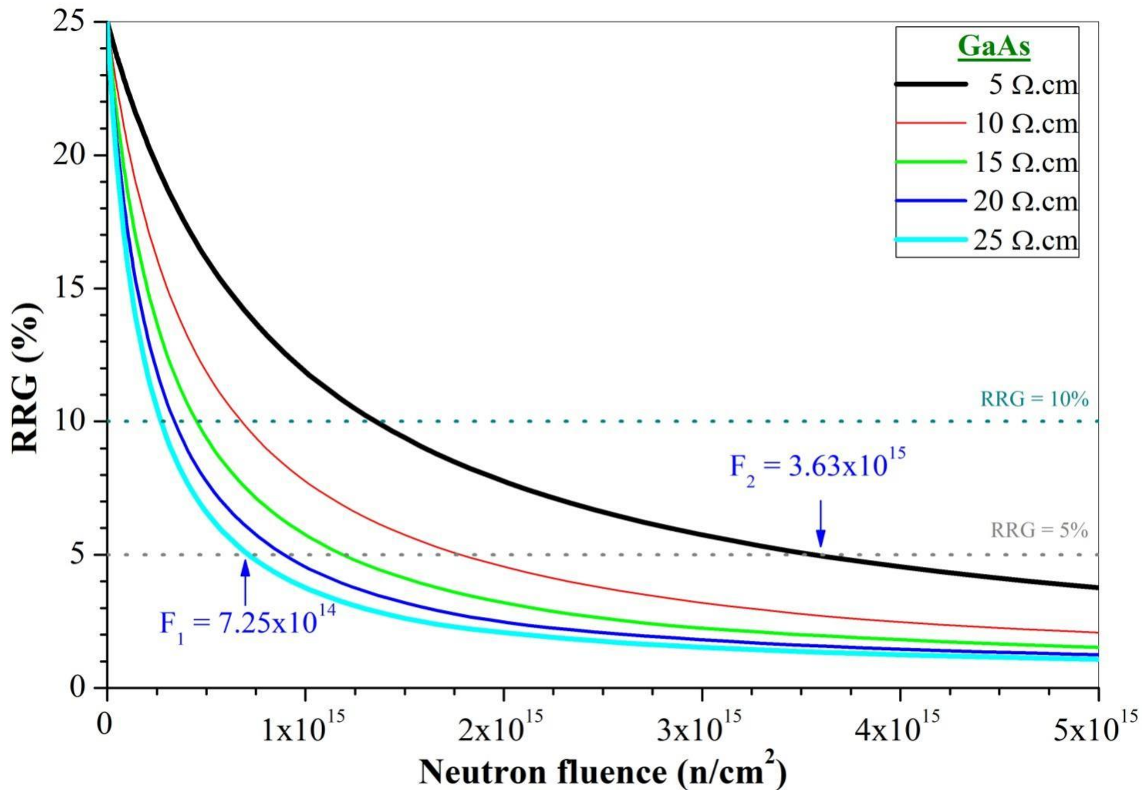

Fig. 4. RRG evolution of the GaAs wafer as a function of the neutron fluence for various cases of initial resistivity.

6.4. Impact of Initial Resistivity on NTD-GaAs Time

Fig. 5 presents the evolution of irradiation time needed to achieve 10% and 5% Radial Resistivity Gradients (RRGs) for five studied cases, with different initial resistivities, irradiated with a thermal neutron flux of $1x10^{12}$ n/cm².s. An interesting correlation emerges between the initial resistivity of the GaAs wafers, their RRGs, and the irradiation time. The curve confirms an inverse proportional relationship: as the initial resistivity increases, the required irradiation time to achieve a specific RRG actually decreases. This observation, along with the fact that even for low-resistivity GaAs, an acceptable RRG (5%) can be achieved within a reasonable irradiation time (one hour at a flux of $1x10^{12}$ n/cm².s), highlights the potential of NTD for improving the uniformity of GaAs wafers, regardless of their initial resistivity.

Further analysis of the data shows that for a desired RRG level, wafers with higher initial resistivity require less irradiation time. This can be attributed to the lower dopant concentration in these wafers. With less dopant initially present, achieving the desired uniformity through NTD requires a smaller increase in dopant concentration, leading to a shorter irradiation time. Additionally, the reduction in RRG is more pronounced for these higher resistivity wafers, highlighting the enhanced effectiveness of the neutron treatment process for GaAs with higher initial resistivity.

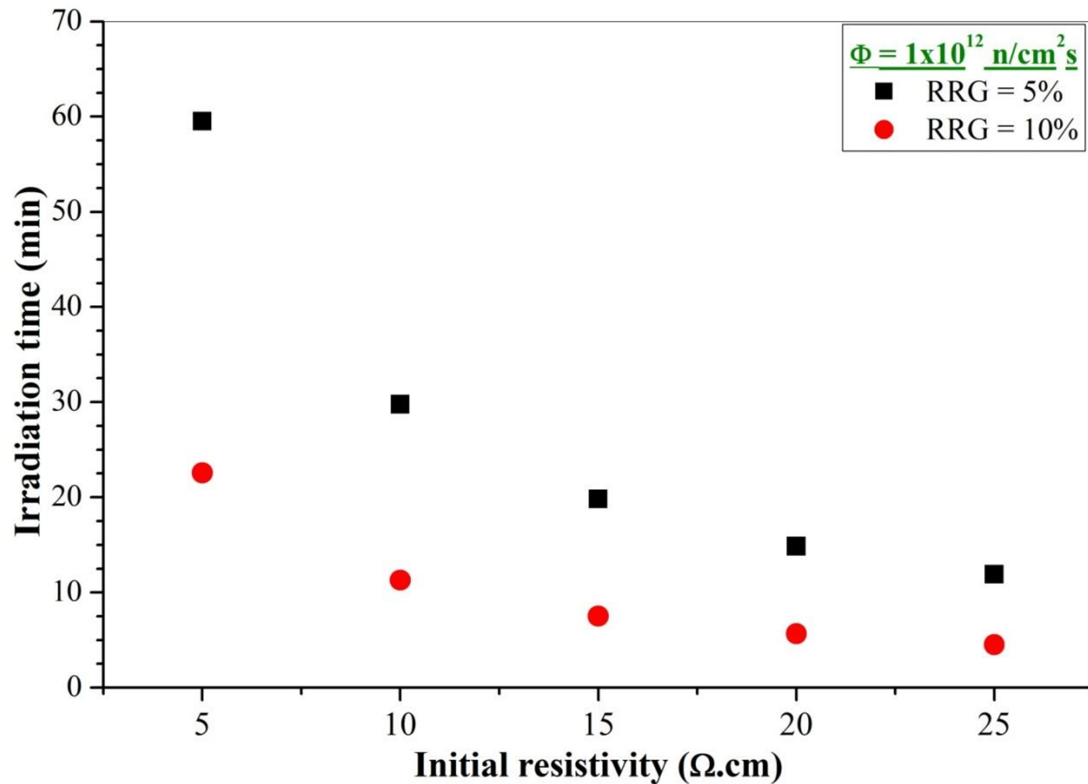

Fig. 5. Evolution of irradiation time required to achieve 5% and 10% RRGs as a function of initial resistivity for GaAs wafers irradiated with a thermal neutron flux of $1\text{x}10^{12}$ n/cm^{2}s.

7. Conclusion

The analysis of the simulation results confirms the effectiveness of NTD in improving the uniformity of dopant concentration within GaAs wafers. Notably, NTD effectively reduces resistivity and Radial Resistivity Gradient (RRG) regardless of the initial resistivity of the wafer. Furthermore, the irradiation time required to achieve a desired RRG is inversely proportional to the initial resistivity. This highlights the potential of NTD for achieving desired electrical properties in GaAs wafers by optimizing their doping profiles, leading to potentially improved device performance.

Acknowledgments

The authors are very grateful to Dr Hocine BENKHARFIA for its help with regard to the SCALE6.1 software.

Conflict of Interest

The authors declare that they have no conflict of interest.

References

1. Tanenbaum M, Mills AD. Preparation of uniform resistivity n-type silicon by nuclear transmutation. *J. Electrochem. Soc*. 1961;108(2):171-176. https://doi.org/10.1149/1.2428036.
2. Mirianashvili ShM, Nanobashvili DI. *Soviet Physics Semiconductors*. 1971;4:1612.
3. Mari B, Navarro FJ, Hernández MA, Riera J. Radiation damage in neutron transmutation doped-InP. *NIM B*. 1996;120:240-243. https://doi.org/10.1016/S0168-583X(96)00517-4.
4. Didik VA, Malkovich RSh, Skoryatina EA, Kozlovski VV. Profiles of transmutation isotopes formed in solids by irradiation with charged particles: Formation, analysis and use. *NIM B*. 2000;160:387-396. https://doi.org/10.1016/S0168-583X(99)00610-2.
5. Labouret A, Cumunel P, Braun JP, Faraggi B. Cellules solaires: les bases de l'énergie photovoltaïque. 5th ed. ETSF, Dunod; 2010. ISBN: 2100555987.
6. Raj V, Haggren T, Wong WW, Tan HH, Jagadish C. Topical Review: Pathways toward cost-effective single-junction III-V solar cells. *J. Phys. D: Appl. Phys*. 2021;55(14):1-41. https://doi.org/10.1088/1361-6463/ac3aa9.

7. SCALE: A Comprehensive Modeling and Simulation Suite for Nuclear Safety Analysis and Design. ORNL/TM-2005/39. Version 6.1, Jun. Available from Radiation Safety Information Computational Center at Oak Ridge National Laboratory as CCC-785; 2011.
8. Greene PD. Transmutation doping of GaAs by thermal neutrons. *Solid State Commun*. 1979;32(2):325-326.
9. Vesaghi MA, Fritzsche H. Neutron transmutation doping of GaAs, cited in: *Guldberg J*, ed. Neutron-Transmutation-Doped Silicon. Plenum Press, New York; 1981:487-488.
10. Garrido J, Castano JL, Piqueras J. Deep centers in neutron-transmutation-doped gallium arsenide. *Solid-State Electron*. 1985;28(10):1039-1043. https://doi.org/10.1016/0038-1101(85)90036-X.
11. Alexiev D, Butcher KSA. Neutron transmutation doping of gallium arsenide. *NIM B*. 1993;83:430-436. https://doi.org/10.1016/0168-583X(93)95867-5.
12. Morvic M, Boháček P, Betko J, Dubecký F, Huran J, Sekáčová M. Electrical properties of semi-insulating GaAs irradiated with neutrons. *NIM B*. 2002;197:240-246. https://doi.org/10.1016/S0168-583X(02)01360-5.
13. Young MH, Hunter AT, Baron R, Marsh OJ, Winston HV, Hart RR. Neutron transmutation doping of p-type czochralski-grown gallium arsenide, cited in: Larrabee RD, ed. Neutron Transmutation Doping of Semiconductor Materials. Plenum Press, New York; 1984:1-20. https://doi.org/10.1007/978-1-4613-2695-3.
14. IAEA report. Neutron Transmutation Doping of Silicon at Research Reactors. IAEA-TECDOC-1681, VIENNA; 2012.
15. Lévy F. Physique et technologie des semi-conducteurs (Traité des matériaux). Edition Broché vol.18; 1994. ISBN: 978-2-88074-272-0.
16. Carbonari AW, Pendl Jr W, Sebastião JR, Saxena RN, Dias MS. An irradiation rig for neutron transmutation doping of silicon in the IEA-R1 research reactor. *NIM B*. 1993;83(1-2):157-162. https://doi.org/10.1016/0168-583X(93)95920-Z.
17. Kim S-H, Hwang J-H, Choi Y-K, Sim B-C. Method of Manufacturing Single Crystal Ingot, and Single Crystal Ingot and Wafer Manufactured Thereby. International Publication No. WO 2012/134092 A2; 2012. https://patents.google.com/patent/WO2012134092A2/en.
18. Park B-G, Sun G-M, Kim M-S. Design Concept of Neutron Irradiation Basket for 12-inch NTD in HANARO. *Transactions of the Korean Nuclear Society Autumn Meeting*, Goyang, Korea, October 24-25, 2019.